JPPIPA 12 (7) (2026)

Jurnal Penelitian Pendidikan IPA

http://jppipa.unram.ac.id/index.php/jppipa/index

Integrated Electrical Resistivity Tomography and SPAC Microtremor for Local Site Response Assessment toward Sustainable Disaster Risk Reduction: A Case Study of Setiling Village, Central Lombok

Syarifatul Ulfah[1*], Muhamad Yamin[1], Bagus Widhi Dharma S.[1]

[1] Department of Civil Engineering, Universitas Qamarul Huda Badaruddin Bagu, Lombok Tengah, Indonesia.

Received: May 19, 2026
Revised: June 12, 2026
Accepted: July 25, 2026
Published: July 31, 2026

Corresponding Author:
Syarifatul Ulfah
syarifa9296@gmail.com

DOI: 10.29303/jppipa.v12i7.15759

Abstract: Local geological conditions strongly influence seismic-wave propagation and earthquake ground response, particularly in heterogeneous volcanic environments. This study aimed to characterize shallow subsurface conditions and assess local seismic site response in Setiling Village, Central Lombok, Indonesia, by integrating two-dimensional Electrical Resistivity Tomography (ERT) using the Wenner–Schlumberger configuration with Spatial Autocorrelation (SPAC)-based microtremor analysis. Three ERT profiles and twenty SPAC measurement points were acquired to evaluate subsurface heterogeneity and near-surface stiffness. The ERT results revealed significant resistivity variations associated with volcanic lithology, weathering intensity, moisture content, and groundwater conditions. Conductive zones (<100 Ωm) were interpreted as highly weathered volcanic deposits, whereas higher resistivity zones (>600 Ωm) represented relatively competent volcanic materials. SPAC-derived Vs30 values ranged from 150 to 525 m/s, corresponding to NEHRP Site Classes C, D, and E. Integrated interpretation demonstrated a consistent relationship between resistivity and Vs30, indicating that progressive volcanic weathering simultaneously reduces electrical resistivity and subsurface stiffness. The integrated ERT–SPAC approach provides a reliable framework for village-scale seismic site characterization, supporting seismic hazard assessment, risk-informed spatial planning, resilient infrastructure development, and disaster risk reduction in tropical volcanic regions.

Keywords: Geoelectrical resistivity, Local site response; Microtremor; Soil vulnerability; Vs30

Introduction

Earthquakes remain one of the most destructive natural hazards in tectonically active regions, causing substantial loss of life, severe damage to infrastructure, and long-term socio-economic disruption. While earthquake magnitude, focal depth, rupture mechanism, and source-to-site distance primarily control the intensity of ground shaking, numerous post-earthquake investigations have demonstrated that local geological conditions significantly influence the spatial variability of earthquake damage through the phenomenon known as local site response (Adhikari et al., 2023; Hayashi et al., 2022; Karagoz et al., 2015). Local site response describes the modification of seismic-wave characteristics as they propagate through shallow subsurface materials with contrasting physical and mechanical properties (Susilo et al., 2023). Variations in lithology (Fadilah et al., 2025), weathering intensity, fracture density, groundwater conditions (Ferdy et al., 2025), and subsurface stiffness may amplify or attenuate seismic waves (Keskinsezer & Dağ, 2019), resulting in markedly different levels of ground shaking within relatively short distances (Ulfah et al., 2021). Therefore,

How to Cite:
Ulfah, S., Yamin, M., & Dharma S., B. W. (2026). Integrated Electrical Resistivity Tomography and SPAC Microtremor for Local Site Response Assessment toward Sustainable Disaster Risk Reduction: A Case Study of Setiling Village, Central Lombok. *Jurnal Penelitian Pendidikan IPA*, *12*(7), 329–347. https://doi.org/10.29303/jppipa.v12i7.15759

understanding the geological factors controlling local site response is essential for reliable seismic hazard assessment, earthquake-resistant engineering design, and disaster risk reduction (Darisma et al., 2020).

Microtremor measurements have become one of the most widely applied passive seismic methods for investigating shallow subsurface conditions because they utilize naturally occurring ambient vibrations without requiring artificial seismic sources (Xie et al., 2023). Owing to their rapid acquisition, non-destructive nature, and cost-effectiveness, microtremor techniques have been extensively used for seismic site characterization and local site response assessment (Cho, 2023). Depending on the acquisition geometry, microtremor observations can provide different types of subsurface information. Single-station measurements are commonly employed to estimate the site's natural frequency and amplification through the Horizontal-to-Vertical Spectral Ratio (HVSR) method (Harsuko et al., 2020), whereas microtremor array measurements, analyzed using the Spatial Autocorrelation (SPAC) method (Subedi et al., 2021), enable the estimation of Rayleigh-wave dispersion curves that can be inverted to obtain one-dimensional shear-wave velocity profiles. Consequently (Cho, 2023), the SPAC method provides a physically based characterization of subsurface dynamic properties and allows reliable estimation of the time-averaged shear-wave velocity in the upper 30 m (Vs30) (Hayashi et al., 2022), which is internationally recognized as the standard parameter for seismic site classification in engineering design codes such as the National Earthquake Hazards Reduction Program (NEHRP) and Eurocode 8 (Building Seismic Safety Council (BSSC), 2000). Because Vs30 reflects the stiffness of near-surface materials, it has been widely adopted to evaluate seismic-wave amplification and classify local site conditions (Prayitno et al., 2026).

Although Vs30 is an effective indicator of subsurface stiffness, it cannot independently explain the geological factors responsible for local site response (Akkaya, 2020). Similar Vs30 values may occur in different geological settings because shear-wave velocity is influenced not only by lithology but also by weathering intensity, porosity, fracture development, and groundwater saturation (Adhikari et al., 2023). Consequently, site classification based solely on Vs30 may oversimplify heterogeneous geological conditions and provide limited information regarding the processes controlling seismic-wave amplification (Ghione et al., 2023). This limitation is particularly important in volcanic terrains, where rapid lateral changes in lithology and tropical weathering produce substantial contrasts in engineering properties over relatively short distances (Caesario et al., 2024).

To complement the dynamic information provided by Vs30, two-dimensional Electrical Resistivity Tomography (ERT) was employed using the Wenner–Schlumberger electrode configuration, which offers balanced sensitivity to both vertical and lateral resistivity variations while maintaining a relatively high signal-to-noise ratio (Żogała et al., 2026). The inverted resistivity models provide detailed information on lithological boundaries, weathered zones, groundwater distribution (Karimah et al., 2022a; Lech et al., 2020; Pazzi et al., 2018; Perrone et al., 2014), and shallow geological structures because electrical resistivity is highly sensitive to mineral composition, pore-fluid conductivity, moisture content, porosity, and weathering intensity (Susilo et al., 2018; Ulfah et al., 2021). Consequently, integrating ERT-derived resistivity models with SPAC-derived Vs30 enables simultaneous evaluation of geological heterogeneity and dynamic soil properties, resulting in a more comprehensive interpretation of local site response than either method alone.

Previous studies have demonstrated the usefulness of geoelectrical investigations and microtremor observations for seismic site characterization (Gemilang et al., 2024; Ghione et al., 2023; Susilo et al., 2018). However, most studies have interpreted resistivity models and Vs30 independently, with resistivity primarily describing lithological conditions and Vs30 representing dynamic site classification (Ryanto et al., 2022). Consequently, limited attention has been given to explaining how geological heterogeneity, particularly volcanic weathering, controls the spatial variability of dynamic site properties. Furthermore, most published investigations focus on regional seismic microzonation at the city or district scale, whereas village-scale studies remain relatively scarce despite their direct relevance to infrastructure planning and community-based disaster mitigation. As a result, local governments often rely on generalized geological maps that cannot adequately represent small-scale variations in shallow subsurface conditions required for engineering applications. These limitations indicate the need for an integrated geological interpretation that quantitatively links resistivity variations with SPAC-derived shear-wave velocity to explain the mechanisms controlling local site response.

Indonesia is one of the world's most seismically active regions because it is located along the convergent boundary between the Indo-Australian and Eurasian tectonic plates. Lombok Island experienced a sequence of destructive earthquakes in 2018 that caused considerable spatial variations in structural damage despite similar distances from the earthquake source (Ulfah et al., 2021). Such variations suggest that local geological conditions significantly influenced ground-motion amplification. Although the 2018 earthquake sequence has been extensively investigated at the regional scale, site-specific studies that explain the relationship between shallow geological conditions and local site response in Central Lombok remain limited. Consequently, local governments and infrastructure planners still rely primarily on regional geological maps and generalized seismic hazard information, which are insufficient to represent small-scale subsurface heterogeneity required for engineering design and village-scale disaster mitigation. According to the Geological Map of the Lombok Sheet (Mangga et al., 1994), Setiling Village is predominantly underlain by Quaternary volcanic deposits consisting of volcanic breccia, tuff, pyroclastic materials, and lava-derived rocks that have undergone different degrees of tropical weathering. These heterogeneous volcanic deposits produce significant contrasts in both electrical resistivity and shear-wave velocity, making the area an appropriate natural laboratory for investigating the relationship between geological conditions and local site response (Hall & Smyth, 2008). Despite its geological complexity and seismic relevance, Setiling Village has not previously been investigated using an integrated geophysical approach capable of comprehensively characterizing both its geological and geophysical conditions. Consequently, the shallow subsurface characteristics controlling local site response remain poorly understood, introducing considerable uncertainty into seismic hazard assessment and engineering site characterization. Reliable site-specific geological and geophysical information is therefore lacking for infrastructure planning and disaster mitigation in Setiling Village. This knowledge gap is particularly important because detailed subsurface characterization is required to support seismic hazard assessment, earthquake-resistant infrastructure design, village-scale spatial planning, and disaster risk reduction. Therefore, this study was undertaken to provide the first integrated geophysical characterization of Setiling Village using two-dimensional Electrical Resistivity Tomography (ERT) and SPAC-derived Vs30, thereby establishing a scientific basis for sustainable infrastructure development and resilient communities.

The novelty of this study does not lie in merely combining geoelectrical and microtremor methods, since such integration has been widely reported in previous studies. Instead, this study develops a geological interpretation framework that quantitatively explains how resistivity variations associated with tropical volcanic weathering, derived from two-dimensional ERT using the Wenner–Schlumberger electrode configuration (Gao et al., 2018; Lech et al., 2020), influence the spatial distribution of SPAC-derived Vs30 and, consequently, local site response at the village scale. Rather than presenting independent resistivity and Vs30 maps, this approach integrates both datasets to identify the geological processes controlling seismic-wave amplification and to improve the interpretation of engineering site conditions in heterogeneous volcanic terrains.

Therefore, this study aims to (1) characterize the shallow subsurface using two-dimensional Electrical Resistivity Tomography with the Wenner–Schlumberger electrode configuration, (2) estimate Vs30 from microtremor array measurements employing the Spatial Autocorrelation (SPAC) method, (3) evaluate the influence of volcanic weathering and resistivity variations on the spatial distribution of SPAC-derived Vs30 and local site response, and (4) develop an integrated geological interpretation for village-scale seismic vulnerability assessment in Setiling Village, Central Lombok. This integrated framework may also serve as a practical approach for assessing local site response in other tropical volcanic regions with similar geological characteristics. The findings are expected to improve the understanding of geological controls on seismic-wave amplification while providing scientific information to support earthquake-resistant infrastructure design, sustainable spatial planning, and disaster risk reduction in volcanic regions with comparable geological characteristics.

Method

Research Location

Figure 1. Research area

This research was conducted in Setiling Village, North Batukliang District, Central Lombok Regency, West Nusa Tenggara Province, Indonesia. The administrative coordinates are 8° 32′ 45.6″ S, 116° 21′ 39.6″ E. In this study, 3-line geoelectric measurements will be used and integrated with 20 microtremor measurement points for microtremor sampling (See Figure 1).

Geology Condition

The study was conducted in Setiling Village, Batukliang Utara District, Central Lombok Regency, West Nusa Tenggara Province, Indonesia. The area is situated within a tectonically active region influenced by the interaction between the Indo-Australian and Eurasian plates, making Lombok Island highly susceptible to earthquake hazards. The 2018 Lombok earthquake sequence demonstrated significant spatial variability in structural damage, indicating that local geological conditions play an important role in controlling seismic-wave amplification and local site response (Pramono et al., 2020).

According to the Geological Map (See Figure 7) of the Lombok Sheet (Mangga et al., 1994), the study area is predominantly underlain by Quaternary volcanic deposits, including volcanic breccia, tuff, pyroclastic deposits, and lava-derived rocks. These materials have experienced different degrees of tropical weathering, producing considerable lateral and vertical heterogeneity in lithology, porosity, moisture content, and mechanical properties. Such geological variability significantly influences both electrical resistivity and shear-wave velocity, making Setiling Village an appropriate location for investigating the relationship between geological conditions and local site response.

Figure 2. Geology of Research Area (Mangga et al., 1994)

The topography of the study area consists of gently undulating to moderately sloping terrain with elevations ranging from approximately 560 to 700 m above sea level. Land use is dominated by agricultural fields, plantations, and scattered residential areas. Increasing infrastructure development in the area highlights the importance of detailed subsurface characterization for supporting seismic hazard assessment (Akbar et al., 2024), earthquake-resistant infrastructure design, and sustainable land-use planning.

Research Workflow

The overall research methodology consisted of four sequential stages: (1) field data acquisition, (2) data processing and inversion, (3) integrated interpretation of geophysical parameters, and (4) seismic site characterization (Figure 2).

The first stage involved the acquisition of two complementary geophysical datasets. Electrical resistivity data were collected using the Electrical Resistivity Tomography (ERT) method with the Wenner–Schlumberger electrode configuration to characterize lithological variations, weathering zones, and shallow geological structures. Simultaneously, ambient vibration data were acquired using microtremor array measurements for estimating shear-wave velocity profiles through the Spatial Autocorrelation (SPAC) method.

The second stage comprised independent processing of each dataset. The apparent resistivity data were inverted using RES2DINV software to generate two-dimensional resistivity models of the subsurface. Microtremor array data were processed using the Geopsy software package to calculate SPAC coefficients and Rayleigh-wave dispersion curves, which were subsequently inverted using the Dinver module to obtain one-dimensional shear-wave velocity profiles and calculate Vs30 values. Because the analysis was based on the Spatial Autocorrelation (SPAC) array method, the workflow focused on Rayleigh-wave dispersion analysis and shear-wave velocity inversion rather than Horizontal-to-Vertical Spectral Ratio (HVSR) parameter estimation. Consequently, fundamental frequency (f_0), amplification factor (A), and seismic vulnerability index (Kg) were not evaluated in this study.

The third stage involved integrating the resistivity models and Vs30 distributions to evaluate the influence of lithological heterogeneity and volcanic weathering on shallow subsurface stiffness. Rather than interpreting each parameter independently, both datasets were analyzed simultaneously to identify geological controls on local site response. Finally, the integrated interpretation was used to classify engineering site conditions and assess local site response characteristics within the study area. The overall workflow is illustrated in Figure 3.

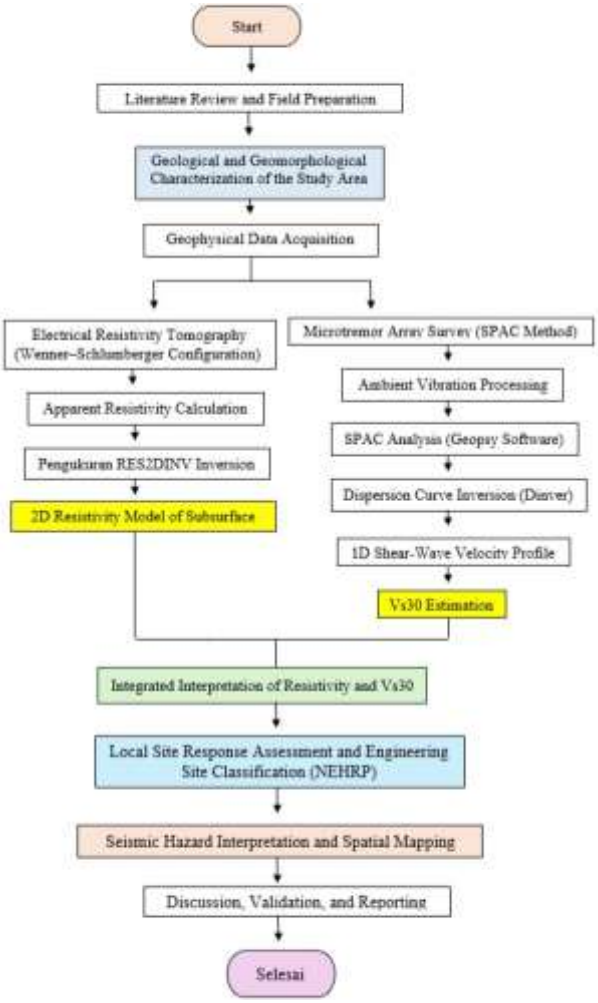

Figure 3. Research workflow

Electrical Resistivity Tomography (ERT) Survey

Electrical Resistivity Tomography (ERT) was employed to characterize the shallow subsurface based on spatial variations in electrical resistivity (Fadillah et al., 2023; Fazriati et al., 2022; Keskinsezer & Dağ, 2019; Omar et al., 2023; Sanny et al., 2023; Syahdilla et al., 2024). The survey was conducted along three two-dimensional profiles, each approximately 1,000 m in length, using the Wenner–Schlumberger electrode configuration. This configuration was selected because it provides balanced sensitivity to both vertical and horizontal resistivity variations while maintaining a relatively high signal-to-noise ratio, making it particularly suitable for imaging heterogeneous volcanic terrains. Each survey line consisted of 21 stainless-steel electrodes installed at 50 m intervals, resulting in a total profile length of approximately 1,000 m. Measurements were acquired using an automatic multi-electrode resistivity imaging system that sequentially injected electrical current through two current electrodes while measuring the resulting potential difference between two potential electrodes. The automated acquisition procedure minimized operator error and ensured consistent data quality throughout the survey. The measured current (I) and potential difference (ΔV) were converted into apparent resistivity (ρ_a) using Ohm's law:

$$\rho_a = K \frac{\Delta V}{I} \quad (1)$$

where ρ_a is the apparent resistivity (Ωm), K is the geometric factor, ΔV is the measured potential difference (V), and I is the injected current (A). For the Wenner–Schlumberger configuration, the geometric factor is expressed as (Loke et al., 2013):

$$K = \pi an\,(n + 1) \quad (2)$$

where A is the electrode spacing (50 m) and n is the spacing factor defining the relative distance between current and potential electrodes.

The apparent resistivity values were subsequently inverted using RES2DINV software based on a smoothness-constrained least-squares inversion algorithm (Karimah et al., 2022b). The inversion process iteratively minimized the root mean square (RMS) error between the observed and calculated apparent resistivity values until convergence was achieved. Data with excessive noise or poor contact resistance were removed during preprocessing to improve inversion stability and model reliability.

Table. 1 Rock Resistivity Value (Telford et al., 1990)

Materials	Resistivity Range (Ωm)
Clay	1–100
Alluvium	10–800
Sand	1–1000
Gravel	100–600
Tuff	20–1000
Basalt	100–10,000
Andesite	170–45,000
Clay	1–100

The resulting two-dimensional resistivity sections were interpreted by considering resistivity contrasts together with the regional geological information of the study area. Low-resistivity zones were interpreted as weathered volcanic materials, clay-rich deposits, or water-saturated layers, whereas moderate resistivity values generally represented partially weathered volcanic deposits (Byrdina et al., 2017; Gao et al., 2018; Longo et al., 2014). High-resistivity anomalies were interpreted as relatively competent volcanic rocks, such as volcanic breccia or lava-derived units, characterized by lower porosity and reduced moisture content. Lithological interpretation followed published resistivity ranges reported in previous geoelectrical studies (See Table 1) and standard references for volcanic environments. With a profile length of approximately 1,000 m and an electrode spacing of 50 m, the estimated investigation depth was approximately within the range of 150–200 m, depending on electrode geometry, subsurface resistivity contrast, and inversion stability. This depth range was considered sufficient to characterize the shallow geological conditions controlling local site response within the study area.

Microtremor Array Survey

Microtremor measurements were conducted to characterize the dynamic properties of the shallow subsurface through passive seismic observations (Harmoko et al., 2026). Unlike active seismic methods, microtremor surveys utilize naturally occurring ambient vibrations generated by natural and anthropogenic sources, including ocean waves, wind, traffic, and human activities. Because no artificial seismic source is required, the method is rapid, non-destructive, cost-effective, and well suited for engineering site characterization and seismic microzonation.

In this study, microtremor array measurements were employed rather than single-station observations because the array technique enables direct estimation of surface-wave dispersion characteristics and provides a physically constrained shear-wave velocity profile. Ambient vibration data were acquired at selected locations representing the principal geological conditions identified from the geoelectrical survey. The array geometry was designed to ensure adequate spatial sampling of Rayleigh waves over the frequency range required to investigate the upper 30 m of the subsurface (Foti et al., 2018).

At each measurement location, ambient vibrations were continuously recorded using synchronized three-component seismometers. The recording duration was adjusted to obtain stable ambient noise signals while minimizing transient disturbances caused by traffic, pedestrians, or other localized vibration sources. Prior to data acquisition, instrument leveling, sensor orientation, and timing synchronization were carefully verified to ensure data consistency throughout the survey. Since this study employed the Spatial Autocorrelation (SPAC) array method rather than single-station Horizontal-to-Vertical Spectral Ratio (HVSR) observations, parameters such as the fundamental frequency (f_0), amplification factor (A), and seismic vulnerability index (Kg) were not evaluated. Instead, the primary output of the SPAC analysis was the Rayleigh-wave dispersion curve, which was subsequently inverted to derive one-dimensional shear-wave velocity profiles and estimate Vs30. Accordingly, the assessment of local site conditions in this study was based on the dynamic properties represented by Vs30 integrated with Electrical Resistivity Tomography (ERT), rather than on HVSR-derived resonance parameters.

SPAC Processing and Shear-Wave Velocity Inversion

The recorded microtremor array data were processed using the Geopsy software package following the Spatial Autocorrelation (SPAC) method originally proposed by Aki (1957). The SPAC method evaluates the spatial correlation of ambient vibration wavefields recorded simultaneously at multiple sensors to estimate the phase velocity of Rayleigh waves over a range of frequencies. The SPAC coefficient is expressed as (Aki, 1957):

$$\rho(r,\omega) = J_0\left(\frac{\omega r}{c(\omega)}\right) \quad (3)$$

Where $\rho(r,\omega)$ is the SPAC coefficient, J_0 is the zero-order Bessel function, ω is the angular frequency (rad s^{-1}), r is the distance between two sensors (m), and c(ω) is the Rayleigh-wave phase velocity corresponding to frequency ω.

The observed SPAC coefficients were subsequently transformed into Rayleigh-wave dispersion curves representing the variation of phase velocity with frequency. These dispersion curves constitute the primary dataset for estimating the shear-wave velocity structure of the subsurface. The dispersion curves were then inverted using the Dinver module integrated within Geopsy. Unlike inversion based solely on HVSR curves, the inversion performed in this study relied directly on the observed Rayleigh-wave dispersion data obtained from the microtremor array. An iterative neighborhood algorithm was employed to search for the one-dimensional shear-wave velocity model that minimized the misfit between observed and theoretical dispersion curves.

The inversion produced one-dimensional shear-wave velocity (Vs) profiles beneath each measurement location. Model selection was based on the lowest misfit values together with the consistency between observed and calculated dispersion curves. Only inversion results exhibiting satisfactory convergence and physically reasonable velocity structures were retained for subsequent interpretation.

Estimation of Vs30

The time-averaged shear-wave velocity within the upper 30 m (Vs30) was calculated from the inverted shear-wave velocity profiles following the recommendation of the National Earthquake Hazards Reduction Program (NEHRP). The Vs30 parameter represents the average propagation velocity of shear waves through the upper 30 m of the subsurface and is widely recognized as the international standard for engineering site classification. The average shear-wave velocity was calculated using (Hanatha et al., 2023):

$$V_{S30} = \frac{30}{\sum_{i=1}^{n} \frac{d_i}{V_{Si}}} \quad (4)$$

Where V_{S30} is the average shear-wave velocity of the upper 30 m (m/s), d_i is the thickness of the (i)-th layer (m), V_{Si} is the shear-wave velocity of the corresponding layer (m/s), and (n) is the number of layers within the upper 30 m depth.

The calculated Vs30 values were subsequently classified according to the NEHRP site classification (See Table 2), which categorizes ground conditions into engineering site classes ranging from hard rock to soft soil. This classification provides an indication of the potential for seismic-wave amplification associated with differences in subsurface stiffness and forms the basis for evaluating local site response (Keskinsezer & Dağ, 2019).

Table. 2 NEHRP Site Classification Based on Vs30 (Building Seismic Safety Council (BSSC), 2000)

Vs30 (m/s)	Site Class	Ground Condition	Vulnerability Level
< 180	SE	Soft Soil	Very High
180–360	SD	Medium Soil	High
360–760	SC	Dense Soil / Soft Rock	Moderate
> 760	SB	Rock	Low

The spatial distribution of Vs30 was generated using the Ordinary Kriging interpolation method within a Geographic Information System (GIS) environment. The resulting Vs30 map was subsequently integrated with the subsurface resistivity model obtained from the Wenner–Schlumberger geoelectrical survey to support the interpretation of lithological variations and near-surface site conditions in the study area.

Data Quality Control

Quality control procedures were applied during both field acquisition and data processing to ensure the reliability of the estimated shear-wave velocity models. During field measurements, ambient vibration records containing transient disturbances such as passing vehicles, strong winds, or temporary anthropogenic noise were identified through visual inspection and excluded from further processing when necessary. During SPAC processing, only frequency bands exhibiting stable coherence between sensors and consistent SPAC coefficients were retained for dispersion analysis. Dispersion curves affected by poor coherence or abnormal phase-velocity trends were discarded to reduce inversion uncertainty.

The reliability of the inversion results was evaluated by comparing the observed and theoretical dispersion curves generated by the final inversion model. Models with relatively low misfit values and good agreement between measured and calculated dispersion curves were considered acceptable. This procedure reduced the non-uniqueness commonly associated with inversion and improved the robustness of the derived shear-wave velocity profiles. The resulting Vs30 values were subsequently integrated with the two-dimensional resistivity models obtained from the Electrical Resistivity Tomography survey to evaluate the relationship between lithological heterogeneity, volcanic weathering, and local site response in Setiling Village.

Result and Discussion

Electrical Resistivity Tomography Results

The Electrical Resistivity Tomography (ERT) survey using the Wenner–Schlumberger electrode configuration successfully imaged the shallow subsurface beneath Setiling Village. Following inversion using the smoothness-constrained least-squares algorithm implemented in RES2DINV, three two-dimensional resistivity sections were produced, revealing substantial lateral and vertical variations in electrical resistivity. These variations primarily reflect differences in lithology, weathering intensity, fracture development, moisture content, and groundwater distribution within the Quaternary volcanic deposits. Lithological interpretation was performed by integrating the inverted resistivity models with the regional geological information of Lombok Island (Mangga et al., 1994) and published resistivity ranges for volcanic environments. Because electrical resistivity is controlled by several physical factors, including mineral composition, pore-fluid conductivity, porosity, and weathering intensity, the resistivity models were interpreted within their geological context rather than as direct indicators of mechanical stiffness. This interpretation approach is consistent with previous ERT investigations in volcanic terrains, where electrical resistivity has been interpreted primarily in terms of lithology, weathering intensity, groundwater conditions, and structural heterogeneity rather than as a direct measure of engineering soil properties (Loke et al., 2013; Reynolds, 2011).

Line 1

The resistivity distribution along Line 1 ranges from approximately 6.77 Ωm to 3596 Ωm, with an RMS error of 4.3%, indicating a reliable inversion result (See Figure 4).

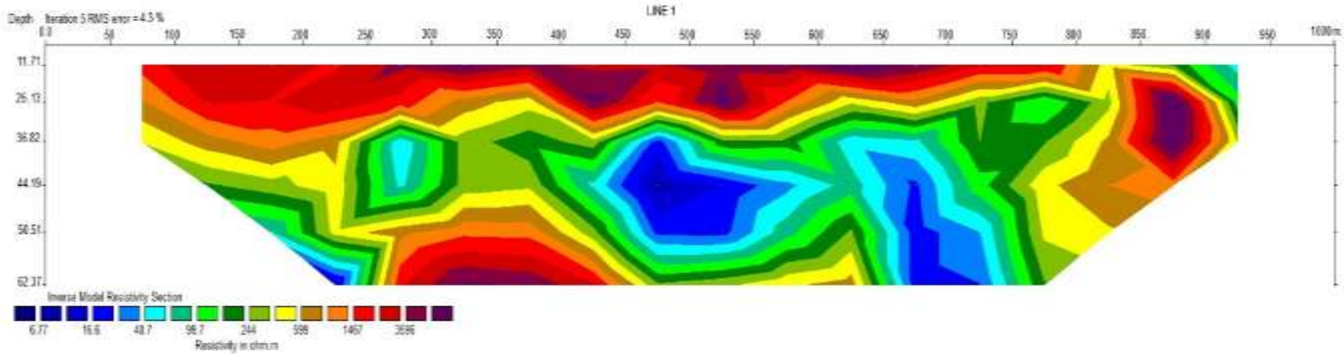

Figure 4. Resistivity of line 1

Low-resistivity anomalies (<100 Ωm) are concentrated within the central portion of the profile at depths between approximately 25 and 60 m. These conductive zones are interpreted as weathered volcanic deposits, clay-rich materials, or water-bearing layers developed through prolonged tropical weathering. Moderate resistivity values (100–600 Ωm) dominate much of the shallow subsurface and likely represent partially weathered volcanic tuff and pyroclastic deposits. In contrast, high-resistivity anomalies (>600 Ωm) occur mainly near the eastern end of the profile and at greater depths, indicating relatively competent volcanic breccia or lava-derived rocks with lower porosity and limited weathering. The transition from competent volcanic materials to weathered volcanic deposits illustrates considerable geological heterogeneity within the profile, which is expected to influence the propagation of seismic waves. Similar resistivity patterns have been reported in volcanic environments by Fadillah et al. (2023), who observed that low-resistivity zones commonly correspond to weathered volcanic deposits enriched in clay minerals and groundwater. Likewise, Reynolds (2011) noted that resistivity contrasts in volcanic terrains generally reflect differences in weathering intensity and pore-fluid distribution.

Line 2

Line 2 exhibits resistivity values ranging from 1.59 Ωm to 23,306 Ωm, with an RMS error of 3.8%, suggesting a high-quality inversion model.

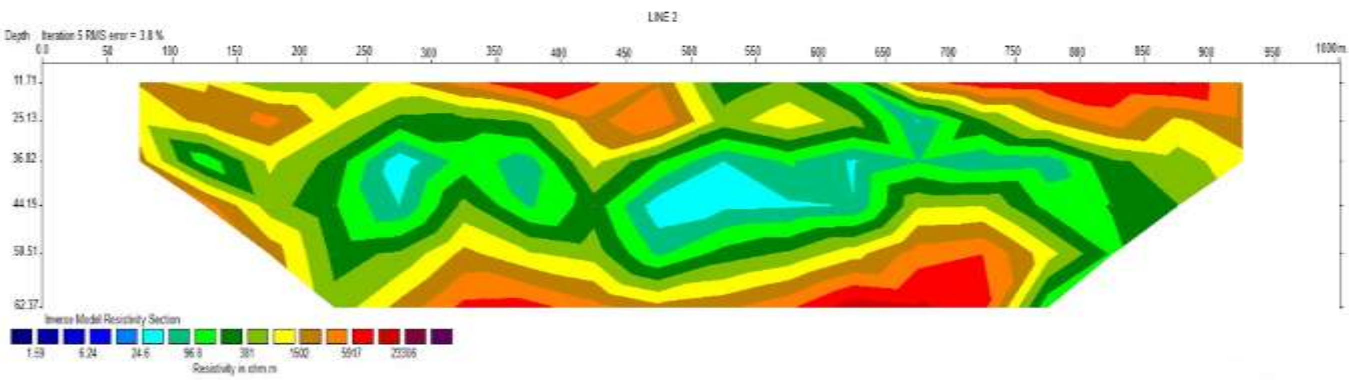

Figure 5. Resistivity of line 2

A broad conductive zone occupies the central section of the profile, extending laterally between approximately 450 and 700 m. These low-resistivity values are interpreted as highly weathered volcanic deposits or saturated fine-grained materials. Intermediate resistivity values characterize the surrounding volcanic deposits, whereas very high resistivity anomalies (>5000 Ωm) are interpreted as compact volcanic bedrock with relatively low degrees of weathering.

Compared with Line 1, Line 2 exhibits greater lateral variation in resistivity, suggesting more complex geological conditions associated with changes in volcanic facies and weathering intensity. Comparable lateral resistivity variations have also been observed by Loke et al. (2013), who demonstrated that abrupt resistivity contrasts often indicate lithological boundaries or structural discontinuities within heterogeneous volcanic deposits.

Line 3

The resistivity values along Line 3 range from approximately 9.7 Ωm to 3496 Ωm, with an RMS error of 4.8%. Compared with the other profiles, Line 3 contains more extensive low-resistivity zones. A large conductive anomaly (<100 Ωm) occurs between 350–800 m at depths of approximately 20–60 m. These low resistivity values suggest thick accumulations of weathered, saturated, and unconsolidated materials. Moderate resistivity values (100–600 Ωm) surround the conductive zone and are interpreted as moderately weathered volcanic deposits. Higher resistivity values (>600 Ωm) are observed mainly in the deeper western and eastern portions of the profile, indicating compact volcanic rocks or more consolidated geological units. The extensive low-resistivity anomaly identified in Line 3 suggests that this profile crosses the most vulnerable subsurface zone among the three survey lines. The occurrence of extensive conductive anomalies is consistent with observations by Keskinsezer and Dağ (2019), who reported that thick weathered and moisture-rich volcanic deposits are commonly associated with reduced subsurface stability and increased geohazard susceptibility.

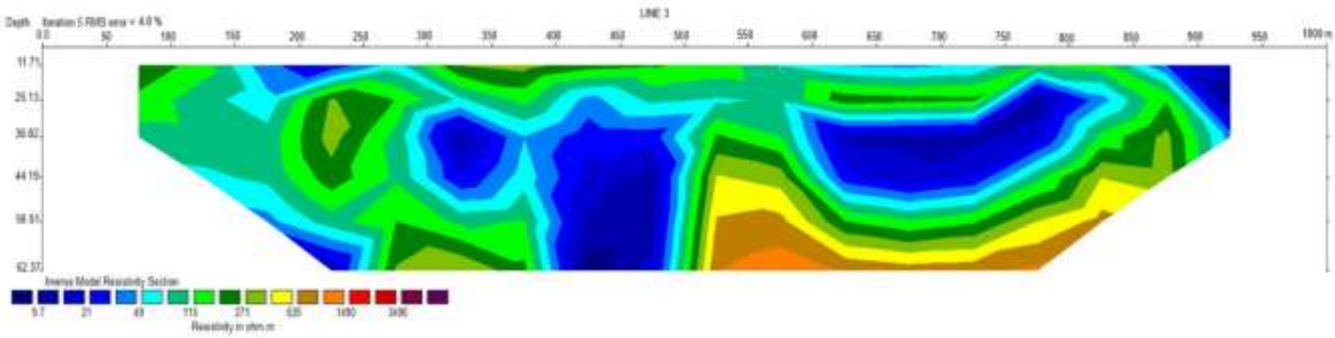

Figure 6. Resistivity of line 3

Overall, the geoelectrical survey results indicate that the subsurface of the area is composed of a combination of weathered volcanic deposits, tuffaceous materials, water-saturated sediments, and compact volcanic bedrock (Mangga et al., 1994). The presence of low-resistivity zones identified consistently along all three survey lines, particularly within the central part of the study area, suggests the occurrence of weak, weathered, and saturated subsurface materials. These deposits are expected to exhibit relatively lower stiffness and may be more susceptible to seismic-wave amplification than the surrounding competent volcanic units. Similar relationships between low electrical resistivity, intense weathering, and groundwater accumulation have been reported by Gao et al. (2018) and Byrdina et al. (2017). These studies demonstrated that progressive volcanic alteration increases pore-fluid conductivity and clay mineral formation, resulting in reduced electrical resistivity. The present study confirms that comparable weathering processes also characterize the volcanic deposits underlying Setiling Village.

Based on the spatial distribution and thickness of the low-resistivity zones, Line 3 exhibits the most extensive conductive anomalies, followed by Line 2, whereas Line 1 is dominated by moderate- to high-resistivity materials that are interpreted as relatively more competent volcanic deposits. These observations suggest that the central portion of the study area contains thicker weathered and potentially water-saturated volcanic materials, reflecting greater geological heterogeneity than the surrounding areas. However, because electrical resistivity primarily reflects lithological characteristics, weathering intensity, and groundwater conditions rather than dynamic soil properties, the geoelectrical results alone are insufficient to evaluate local site response and soil vulnerability. Although the geoelectrical models successfully delineate lithological heterogeneity, resistivity alone cannot directly quantify dynamic soil behavior because electrical conductivity is influenced by several non-mechanical factors, including groundwater salinity, clay mineral content, and pore-fluid saturation (Reynolds, 2011). Therefore, an additional geophysical parameter representing subsurface stiffness is required to evaluate engineering site conditions more reliably.

To characterize the dynamic behavior of the shallow subsurface, 20 microtremor array measurements employing the Spatial Autocorrelation (SPAC) method were conducted throughout the study area, including locations corresponding to the three geoelectrical survey lines. The SPAC analysis produced one-dimensional shear-wave velocity profiles from which the average shear-wave velocity in the upper 30 m (Vs30) was calculated. Since this study employed the

SPAC array method rather than single-station Horizontal-to-Vertical Spectral Ratio (HVSR) observations, parameters such as the fundamental frequency (f_0), amplification factor (A), and seismic vulnerability index (Kg) were not evaluated. Instead, the primary output of the SPAC analysis was Vs30, which provides a robust indicator of near-surface stiffness and seismic site conditions. Unlike HVSR, which primarily evaluates resonance characteristics through dominant frequency and amplification, SPAC directly estimates shear-wave velocity profiles required for calculating Vs30, making it more suitable for quantitative engineering site classification.

The integrated interpretation of the ERT-derived resistivity models and SPAC-derived Vs30 values was subsequently used to evaluate local site response and develop the Soil Vulnerability Zonation Map of Setiling Village. Areas characterized by relatively low resistivity together with low Vs30 values were interpreted as zones of higher seismic vulnerability because they represent weathered volcanic deposits with reduced stiffness and a greater potential for ground-motion amplification. Conversely, areas exhibiting higher resistivity and higher Vs30 values were interpreted as relatively competent volcanic materials with lower susceptibility to seismic amplification. Although previous studies have successfully applied either Electrical Resistivity Tomography (ERT) to characterize lithological heterogeneity (Fadillah et al., 2023) or microtremor techniques such as the Horizontal-to-Vertical Spectral Ratio (HVSR) to evaluate seismic site conditions (Akbar et al., 2024), these approaches generally interpret geological and dynamic properties independently. Consequently, they provide only partial information regarding the processes controlling local site response.

By integrating ERT-derived lithological information with SPAC-derived shear-wave velocity (Vs30), the present study simultaneously evaluates geological heterogeneity, volcanic weathering, and near-surface stiffness within a single interpretation framework. This integrated approach reduces interpretation uncertainty by linking electrical and dynamic subsurface properties, thereby providing a more reliable basis for village-scale seismic site characterization and soil vulnerability assessment than single-method investigations. The resulting interpretation provides valuable scientific support for earthquake-resistant infrastructure planning, sustainable land-use management, and disaster risk reduction in Setiling Village.

Microtremor (SPAC–Vs30) Results

To complement the geological information obtained from the Electrical Resistivity Tomography (ERT) survey, a microtremor array investigation based on the Spatial Autocorrelation (SPAC) method was conducted to characterize the dynamic properties of the shallow subsurface. A total of 20 microtremor measurement points were distributed across Setiling Village and strategically positioned to correspond with the three ERT survey lines (Tabel 3). This survey configuration enabled direct comparison between lithological variations identified from the resistivity models and the dynamic characteristics represented by the average shear-wave velocity of the upper 30 m (Vs30).

Tabel 3. Summary of Vs30 Measurements and Site Classification

Point	Elevation (m)	Vs30 (m/s)	Site Class	Ground Condition
ST01	685	525	C	Weathered volcanic
ST02	662	502	C	Weathered volcanic
ST03	658	498	C	Dense soil
ST04	655	487	C	Dense soil
ST05	635	483	C	Dense soil
ST06	620	460	C	Dense soil
ST07	580	435	C	Dense soil
ST08	565	426	C	Dense soil
ST09	553	398	C	Dense soil
ST10	490	355	D	Medium-dense soil
ST11	450	331	D	Medium-dense soil
ST12	430	325	D	Medium-dense soil
ST13	405	310	D	Medium-dense soil
ST14	430	346	D	Medium-dense soil
ST15	350	250	D	Soft soil
ST16	410	324	D	Medium-dense soil
ST17	305	190	D	Soft soil
ST18	290	185	D	Soft soil
ST19	290	150	E	Very soft soil
ST20	195	165	E	Very soft soil

The recorded ambient vibration data were processed using the Geopsy software package. SPAC coefficients were calculated from synchronized three-component recordings and subsequently transformed into Rayleigh-wave dispersion curves. The dispersion curves were inverted using the Dinver module to obtain one-dimensional shear-wave velocity profiles beneath each measurement point. The Vs30 values were then calculated from the inverted velocity models following the NEHRP recommendation, providing a standardized measure of near-surface stiffness for engineering site classification. Unlike the single-station Horizontal-to-Vertical Spectral Ratio (HVSR) method, the Spatial Autocorrelation (SPAC) array technique directly estimates Rayleigh-wave dispersion and allows inversion of shear-wave velocity profiles. Consequently, SPAC provides a more robust basis for calculating Vs30 and engineering site classification in heterogeneous volcanic environments.

The estimated Vs30 values range from 150 to 525 m/s. The Vs30 distribution observed in this study is generally consistent with previous microtremor investigations conducted in volcanic environments. For example, Cho (2023) demonstrated that the SPAC method provides reliable estimation of Rayleigh-wave dispersion and Vs30 at stiff-soil and rock sites, whereas Hayashi et al. (2022) reported that SPAC-derived shear-wave velocity models provide physically constrained subsurface stiffness suitable for engineering site classification. The Vs30 values obtained in Setiling Village therefore confirm that SPAC is capable of resolving significant spatial variations in volcanic weathering and shallow subsurface stiffness. The estimated Vs30 values range from 150 to 525 m/s, indicating considerable spatial variability in the mechanical properties of the shallow subsurface (Table 3). The Vs30 distribution observed in this study is generally consistent with previous microtremor investigations conducted in volcanic environments. Based on the NEHRP classification, the study area is represented by three engineering site classes: Site Class C (Dense Soil/Soft Rock), Site Class D (Medium Soil), and Site Class E (Soft Soil). The highest Vs30 values were observed at ST01–ST09, where velocities vary between 398 and 525 m/s. These locations are predominantly situated in the higher-elevation parts of Setiling Village and are classified as Site Class C. According to field observations and the corresponding geoelectrical interpretation, these sites are underlain by relatively dense volcanic deposits and weathered volcanic rock with comparatively high mechanical stiffness. The higher shear-wave velocities indicate that these materials are capable of transmitting seismic energy more efficiently while exhibiting relatively limited ground-motion amplification compared with softer deposits.

A gradual reduction in Vs30 is observed toward the intermediate part of the study area. Measurement points ST10–ST18 exhibit velocities ranging from 185 to 355 m/s, corresponding to Site Class D. These locations are interpreted as being underlain by moderately weathered volcanic deposits, pyroclastic materials, and medium-dense soils. The reduction in shear-wave velocity reflects the progressive effects of weathering, which increase porosity, reduce material cohesion, and decrease overall soil stiffness. Consequently, Site Class D represents transitional ground conditions with a greater potential for seismic-wave amplification than Site Class C.

The lowest Vs30 values occur at ST19 and ST20, where measured velocities are 150 m/s and 165 m/s, respectively. These locations are classified as Site Class E, representing very soft soil conditions. Such low shear-wave velocities indicate highly weathered and unconsolidated near-surface materials with low shear strength. These deposits are expected to experience the greatest amplification of seismic waves because their low stiffness promotes prolonged ground shaking and larger deformation during earthquake loading.

The spatial distribution of Vs30 reveals a distinct trend across the study area. Higher velocities are concentrated within the elevated northern and western sectors, whereas progressively lower velocities occur toward the central and lower-elevation areas. This pattern reflects the geological evolution of Setiling Village, where relatively competent volcanic rocks dominate the higher terrain, while thicker accumulations of weathered volcanic deposits and unconsolidated materials occupy lower topographic positions. Although elevation itself does not directly control Vs30, the observed topographic pattern corresponds closely with the distribution of geological materials and weathering intensity identified in the ERT survey.

The engineering site classification further emphasizes the predominance of Site Class C throughout much of the study area, indicating that dense volcanic deposits constitute the principal shallow subsurface material. However, the occurrence of Site Classes D and E within the central and lower-elevation sectors demonstrates significant local variations in soil stiffness. These variations highlight the heterogeneous nature of tropical volcanic deposits, where differences in weathering intensity and groundwater conditions produce substantial contrasts in shear-wave velocity over relatively short distances. Similar engineering site classifications have been reported in previous studies. Ghione et al. (2023) observed that lower Vs30 values are generally associated with weathered and unconsolidated deposits, whereas higher Vs30 values correspond to competent bedrock. Likewise, Adhikari et al. (2023) demonstrated that spatial variations in Vs30 effectively represent differences in seismic site conditions and local amplification potential.

Comparison between the SPAC-derived Vs30 distribution and the ERT resistivity models reveals a high degree of spatial consistency. Locations characterized by relatively high resistivity generally coincide with higher Vs30 values and Site Class C, indicating compact volcanic materials with greater mechanical competence. Conversely, areas exhibiting low electrical resistivity correspond predominantly to Site Classes D and E, where lower Vs30 values indicate weathered, moisture-rich, and unconsolidated volcanic deposits. Although resistivity and shear-wave velocity represent different physical properties, both datasets consistently identify the same zones of geological heterogeneity.

The observed correspondence between electrical resistivity and SPAC-derived Vs30 extends previous studies that generally investigated these parameters separately. Keskinsezer and Dağ (2019) combined resistivity, MASW, and microtremor methods to investigate landslide-prone areas and demonstrated that integrating multiple geophysical datasets substantially improves subsurface interpretation compared with a single method. Similarly, Fadillah et al. (2023) emphasized that ERT effectively delineates lithological heterogeneity in volcanic terrains. In the present study, however, the integration of ERT with SPAC-derived Vs30 enables simultaneous evaluation of lithological conditions and dynamic soil stiffness. The correspondence between these independent datasets demonstrates that volcanic weathering exerts a strong influence on both the electrical and mechanical characteristics of the shallow subsurface. Progressive weathering increases porosity, promotes groundwater retention, and alters the original volcanic rock fabric.

These processes reduce electrical resistivity through enhanced pore-fluid conductivity while simultaneously decreasing shear-wave velocity owing to reduced material stiffness. Consequently, the observed decrease in Vs30 within the central part of the study area is consistent with the presence of conductive weathered materials identified by the ERT survey. Similar relationships between volcanic weathering and resistivity reduction have been reported by Gao et al. (2018), who showed that hydrothermal alteration and groundwater infiltration substantially decrease electrical resistivity. The present study further demonstrates that these weathering processes also reduce shear-wave velocity, indicating that electrical and dynamic properties evolve simultaneously during volcanic weathering.

From an engineering perspective, the predominance of Site Classes C and D indicates that most of Setiling Village is underlain by dense to moderately dense volcanic deposits with moderate site conditions. Nevertheless, the localized occurrence of Site Class E identifies areas where very soft soil deposits may significantly amplify seismic ground motion. These zones therefore require greater consideration in seismic hazard assessment, foundation design, and land-use planning.

Overall, the SPAC analysis successfully characterized the dynamic behavior of the shallow subsurface and demonstrated substantial spatial variability in shear-wave velocity across Setiling Village. When integrated with the ERT interpretation, the Vs30 distribution confirms that variations in tropical volcanic weathering strongly influence the mechanical properties of near-surface materials. The complementary nature of both datasets provides a robust basis for evaluating local site response and establishes the foundation for the integrated geological interpretation and soil vulnerability assessment presented in the following section. Unlike the study of Akbar et al. (2024), which evaluated seismic vulnerability using the Horizontal-to-Vertical Spectral Ratio (HVSR) approach based on resonance parameters such as dominant frequency (f_0), amplification factor (A_0), and seismic vulnerability index (Kg), the present study employed the Spatial Autocorrelation (SPAC) array method. SPAC directly estimates Rayleigh-wave dispersion and derives shear-wave velocity profiles for calculating Vs30, providing a physically constrained representation of subsurface stiffness.

Furthermore, integrating SPAC-derived Vs30 with Electrical Resistivity Tomography (ERT) enables simultaneous assessment of geological heterogeneity and dynamic site conditions, offering a more comprehensive framework for evaluating local site response in heterogeneous volcanic terrains than resonance-based HVSR analysis alone. Consequently, the proposed ERT–SPAC framework provides both geological and engineering information simultaneously, whereas HVSR-based interpretation primarily focuses on resonance characteristics.

Integrated Discussion: ERT, SPAC-Derived Vs30, Local Site Response, and Soil Vulnerability

The integration of Electrical Resistivity Tomography (ERT) and SPAC-derived shear-wave velocity (Vs30) provides a comprehensive characterization of the shallow subsurface conditions controlling local site response in Setiling Village. Unlike previous studies that applied either electrical resistivity imaging (Fadillah et al., 2023; Gao et al., 2018) or microtremor techniques independently (Akbar et al., 2024; Cho, 2023), the present study integrates two-dimensional ERT and SPAC-derived Vs30 into a unified interpretation framework. This approach enables simultaneous evaluation of lithological heterogeneity, volcanic weathering, groundwater influence, and dynamic soil stiffness, thereby reducing the ambiguity commonly associated with single-method investigations (Kadri et al., 2025). The combined analysis enables simultaneous evaluation of lithological heterogeneity, degrees of volcanic alteration, groundwater influence, and near-surface stiffness. The resulting integrated interpretation is presented in the Soil Vulnerability Assessment Map (Figure 7), which synthesizes electrical resistivity, SPAC-derived Vs30, engineering site classification, topographic setting, and geological interpretation into a unified framework for assessing local site response and seismic soil vulnerability.

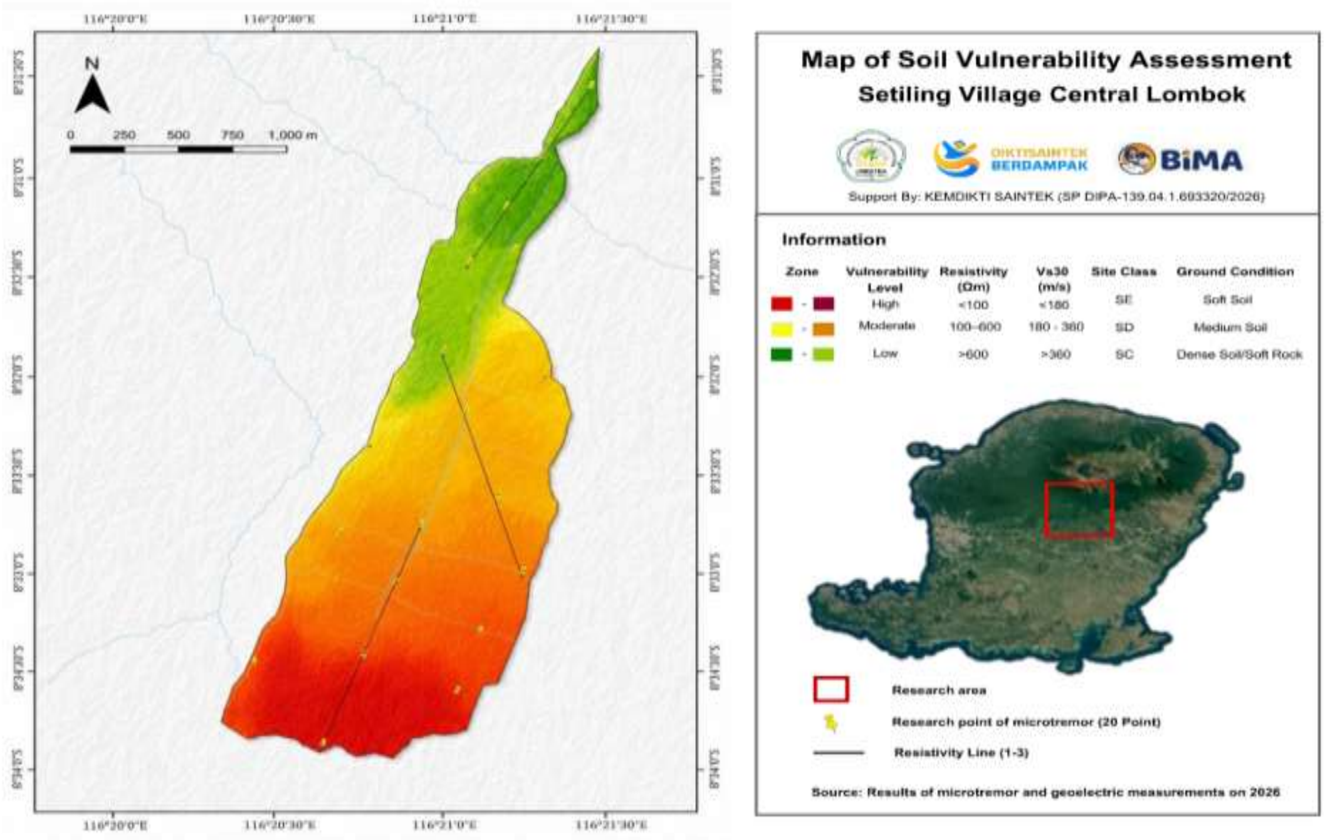

Figure 7. Soil Vulnerability Assessment Map of Setiling Village, Central Lombok

Similar integrated geological zonation has been reported in volcanic environments by Keskinsezer and Dağ (2019), although the present study further incorporates SPAC-derived Vs30 for engineering site classification.

The ERT survey consistently identifies three principal subsurface domains throughout the study area. Low-resistivity zones (<100 Ωm) correspond to highly altered volcanic deposits containing abundant clay minerals and elevated groundwater content. Intermediate resistivity values (100–600 Ωm) represent moderately altered volcanic tuffs and pyroclastic deposits, whereas high-resistivity materials (>600 Ωm) indicate relatively competent volcanic breccia and lava-derived rocks with lower porosity and limited alteration. These lithological variations are consistent with the Quaternary volcanic deposits mapped by Mangga et al. (1994) and reflect progressive modification of volcanic materials under tropical environmental conditions.

The SPAC-derived Vs30 distribution exhibits a spatial pattern that closely agrees with the resistivity models. Higher Vs30 values (398–525 m/s), corresponding to Site Class C, occur predominantly within the northern part of the study area and indicate dense volcanic soil and weathered volcanic rock with relatively high stiffness. Intermediate Vs30 values (185–355 m/s), classified as Site Class D, are mainly distributed across the central sector where volcanic deposits have experienced moderate alteration. The lowest Vs30 values (150–165 m/s), corresponding to Site Class E, occur in the southern sector where thick accumulations of highly weathered and unconsolidated volcanic deposits dominate the shallow subsurface. The Vs30 range obtained in Setiling Village (150–525 m/s This range is comparable to those reported in volcanic terrains of Yogyakarta (Hanatha et al., 2023), where Vs30 values varied between approximately 160 and 520 m/s, indicating similar degrees of weathering despite differences in geological setting. Although the geological settings differ, the similarity of the observed Vs30 pattern suggests that weathering exerts a fundamental control on shallow subsurface stiffness across different volcanic environments.

The strong spatial agreement between the ERT models and the Vs30 distribution indicates that volcanic alteration is the principal geological process governing both the electrical and dynamic characteristics of the shallow subsurface. Progressive alteration increases fracture density, porosity, clay mineral content, and groundwater infiltration, thereby enhancing pore-fluid conductivity and reducing electrical resistivity. Simultaneously, deterioration of the volcanic rock framework decreases shear modulus and material stiffness, resulting in lower shear-wave velocity.

Consequently, zones that have undergone more intensive alteration consistently exhibit both low resistivity and low Vs30, whereas relatively intact volcanic rocks retain higher resistivity together with greater shear-wave velocity. This relationship provides a physical explanation linking geological evolution with variations in local site response. Overall, the integrated interpretation reveals three principal relative site response condition zones that extend systematically from north to south across Setiling Village. Rather than occurring randomly, these zones closely follow variations in lithology, subsurface stiffness, and topographic position, demonstrating that geological evolution exerts a primary control on seismic site conditions.

The northern part of the study area is classified as a Low Vulnerability Zone, where resistivity generally exceeds 600 Ωm and Vs30 is greater than approximately 360 m/s (Site Class C). This sector is interpreted as being underlain by relatively competent volcanic breccia and lava-derived rocks together with dense volcanic deposits that retain high mechanical stiffness and low porosity. Consequently, seismic-wave amplification is expected to be relatively limited, making this area the most favorable location for future infrastructure development. Similar spatial zonation has also been reported by Adhikari et al. (2023), who demonstrated that spatial variability in Vs30 provides an effective basis for seismic microzonation. Nevertheless, the present study extends this concept by integrating resistivity-derived lithological information, enabling the identified vulnerability zones to be interpreted not only from dynamic properties but also from the underlying geological processes.

The central part of the study area represents a Moderate Vulnerability Zone, characterized by resistivity values between 100 and 600 Ωm and Vs30 ranging from 180 to 360 m/s (Site Class D). This transitional zone consists predominantly of moderately altered volcanic tuffs and pyroclastic deposits whose engineering properties have been partially reduced through geological alteration. Although these materials remain capable of supporting engineering structures, their intermediate stiffness indicates a greater potential for local seismic-wave amplification than the northern sector. Accordingly, engineering development within this zone should be supported by detailed geotechnical investigation, appropriate foundation design, and site-specific seismic analysis.

The southern part of Setiling Village constitutes the High Vulnerability Zone, where resistivity values are generally below 100 Ωm and Vs30 is less than 180 m/s (Site Class E). This sector is interpreted as being underlain by thick accumulations of highly altered, moisture-rich, clay-bearing, and unconsolidated volcanic deposits. The coexistence of low electrical resistivity and very low shear-wave velocity indicates weak subsurface materials with limited mechanical competence and a high potential for seismic-wave amplification. During future earthquake events, these deposits are expected to experience stronger ground motion than the surrounding volcanic formations. Therefore, this sector may require greater consideration in future seismic assessment and land-use planning, earthquake-resistant engineering, and risk-sensitive land-use planning.

The systematic transition from low vulnerability in the north to high vulnerability in the south reflects the geological evolution of the volcanic terrain rather than random spatial variability. Higher-elevation areas remain dominated by relatively competent volcanic formations that have undergone limited alteration, whereas lower-elevation areas contain thicker accumulations of weak volcanic deposits that have experienced prolonged chemical alteration and groundwater infiltration. These long-term geological processes progressively reduce both electrical resistivity and shear-wave velocity, thereby increasing the susceptibility of the near-surface materials to seismic-wave amplification. The consistency observed between the ERT models, Vs30 distribution, and vulnerability zonation demonstrates that geological conditions exert a fundamental control on local site response throughout the study area.

The results further demonstrate that neither electrical resistivity nor Vs30 alone is sufficient to comprehensively evaluate seismic site conditions. Electrical resistivity primarily reflects lithological composition, groundwater distribution, moisture content, and alteration intensity, whereas Vs30 represents the dynamic stiffness governing seismic-wave propagation. Considered independently, each parameter provides only partial information regarding subsurface characteristics. Their integration substantially reduces interpretation uncertainty by linking geological conditions with dynamic soil behavior, thereby providing a more reliable basis for engineering site classification and seismic hazard assessment. This finding highlights the principal contribution of the present study. Previous investigations generally relied on either electrical resistivity or microtremor measurements separately to characterize shallow subsurface conditions (Akbar et al., 2024; Fadillah et al., 2023). By integrating ERT and SPAC-derived Vs30, the present study establishes a process-based interpretation linking volcanic weathering, lithological variability, electrical properties, and dynamic stiffness within a single framework. Such integration provides a more reliable basis for engineering site classification and village-scale seismic microzonation than single-method investigations.

From an engineering perspective, the soil vulnerability zonation derived from the integrated ERT–SPAC analysis provides practical guidance for infrastructure planning and disaster risk reduction. Areas classified as Low Vulnerability are generally suitable for future development because of their relatively competent subsurface conditions and lower amplification potential. Moderate Vulnerability areas require detailed geotechnical investigations before construction to ensure that foundation systems are compatible with local ground conditions. In contrast, High Vulnerability areas should receive the highest priority in spatial planning, foundation design, earthquake-resistant construction, and disaster preparedness because of their elevated susceptibility to strong ground shaking associated with weak volcanic deposits.

The integrated interpretation demonstrates that combining ERT and SPAC-derived Vs30 provides a more comprehensive evaluation of local site response than interpreting either dataset independently. The complementary relationship between electrical resistivity and shear-wave velocity enables geological heterogeneity, alteration intensity, and near-surface stiffness to be evaluated simultaneously, thereby reducing uncertainty in engineering site characterization. This process-based interpretation extends beyond conventional geophysical mapping by explaining how variations in volcanic alteration influence both the electrical and mechanical behaviour of the shallow subsurface. Most previous investigations focused either on geoelectrical characterization (Fadillah et al., 2023; Gao et al., 2018) or microtremor-based seismic site classification (Akbar et al., 2024; Cho, 2023; Hayashi et al., 2022). In contrast, the present study integrates two-dimensional ERT imaging with SPAC-derived Vs30 to simultaneously evaluate lithological variability, weathering intensity, and engineering site conditions within a tropical volcanic environment. This integrated framework reduces ambiguity associated with single-method interpretation and provides a more reliable basis for seismic microzonation and disaster mitigation at the village scale.

Beyond its application to Setiling Village, the proposed ERT–SPAC integration framework can be adapted to other tropical volcanic regions characterized by heterogeneous weathering conditions. The methodology therefore contributes not only to local seismic hazard assessment but also provides a transferable approach for regional engineering geological investigations. The practical applicability of this framework demonstrates that integrated near-surface characterization can support evidence-based decision making for sustainable regional development. These findings contribute directly to the achievement of Sustainable Development Goal (SDG) 11: Sustainable Cities and Communities by providing scientific evidence for risk-informed spatial planning, resilient infrastructure development, and disaster risk reduction. The village-scale soil vulnerability assessment provides practical guidance for identifying areas requiring different engineering strategies and mitigation priorities, thereby supporting sustainable infrastructure development and strengthening community resilience in earthquake-prone volcanic environments. Overall, the integrated ERT–SPAC methodology establishes a robust framework for village-scale seismic site characterization and offers an approach that can be applied to other tropical volcanic regions with comparable geological settings.

Conclusion

This study characterized shallow subsurface conditions and relative seismic site characteristics in Setiling Village, Central Lombok, Indonesia, through the integration of two-dimensional Electrical Resistivity Tomography (ERT) using the Wenner–Schlumberger configuration and SPAC-based microtremor analysis. The combined interpretation of electrical resistivity and shear-wave velocity (Vs30) provides complementary information regarding subsurface heterogeneity, material stiffness, and variations in local seismic site conditions that cannot be adequately described by either method individually. The ERT results indicate substantial spatial variations in subsurface resistivity associated with differences in volcanic lithology, weathering intensity, moisture conditions, and groundwater-related variations. Low-resistivity zones are interpreted as weathered and moisture-influenced volcanic materials, whereas higher resistivity zones are associated with relatively less altered and more competent volcanic deposits. Among the three investigated profiles, Line 3 presents the most extensive conductive anomalies, indicating a wider distribution of heterogeneous and weathered subsurface materials compared with Lines 1 and 2. The SPAC-derived Vs30 analysis reveals spatial variations in near-surface stiffness, with estimated values ranging from 150 to 525 m/s. Based on the NEHRP site classification, the study area consists of Site Class C, Site Class D, and localized Site Class E conditions. Higher Vs30 values are mainly distributed in the northern and elevated sectors, indicating relatively stiffer subsurface materials, whereas lower Vs30 values are concentrated in the central to southern sectors, reflecting softer and more weathered near-surface materials. The integrated interpretation of ERT and Vs30 data shows a consistent spatial correspondence between electrical and dynamic subsurface properties. Higher resistivity zones generally coincide with higher Vs30 values, while conductive zones tend to be associated with lower Vs30 values. This relationship indicates that variations in volcanic weathering, material alteration, compaction conditions, and moisture content influence both the electrical response and mechanical characteristics of shallow subsurface materials, contributing to spatial differences in local seismic site conditions. And the integrated geophysical assessment identifies three relative seismic site condition zones within Setiling Village. The northern sector is characterized by relatively competent subsurface conditions associated with higher resistivity and Vs30 values. The central sector represents transitional conditions related to moderately weathered volcanic materials with intermediate stiffness. The southern sector exhibits relatively softer subsurface conditions, where lower resistivity and lower Vs30 values indicate materials with reduced stiffness and potentially greater sensitivity to seismic-wave amplification. The main contribution of this study is the establishment of an integrated interpretation framework that links resistivity variations, SPAC-derived Vs30 distribution, and geological conditions for village-scale subsurface characterization in a heterogeneous tropical volcanic environment. This framework provides additional understanding of the relationship between volcanic weathering processes and variations in shallow subsurface physical and dynamic properties. The results provide preliminary scientific information that can support earthquake risk-informed spatial planning, infrastructure development, and sustainable land-use management in Setiling Village. However, the identified seismic site condition zones represent relative variations in subsurface characteristics and should not be considered as substitutes for detailed engineering investigations. Further validation through geological and geotechnical measurements, including borehole logging, Standard Penetration Test (SPT), Cone Penetration Test (CPT), laboratory analysis, and complementary seismic methods such as Multichannel Analysis of Surface Waves (MASW) or active seismic refraction, is recommended to improve subsurface characterization and reduce uncertainty. Overall, the integrated ERT–SPAC approach provides a practical framework for shallow subsurface characterization and local seismic site assessment in tropical volcanic regions. The findings contribute to Sustainable Development Goal (SDG) 11 by providing scientific information that supports risk-informed spatial planning, resilient infrastructure development, and disaster risk reduction strategies. With appropriate geological and geotechnical validation, this framework may be applicable to other volcanic regions with comparable geological settings.

Acknowledgments

The authors sincerely acknowledge Universitas Qamarul Huda Badaruddin Bagu for its institutional support, research facilities, and administrative assistance throughout this study. Appreciation is also extended to the local government and the community of Setiling Village, West Lombok Regency, Indonesia, for granting access to the study area and facilitating the field investigations. The authors are grateful to their colleagues and field assistants for their valuable support during the geophysical data acquisition, processing, and interpretation. Their contributions were essential to the successful completion of this research.

Author Contributions

Conceptualization, Syarifatul Ulfah; methodology, Syarifatul Ulfah; software, Syarifatul Ulfah; validation, Syarifatul Ulfah, Muhamad Yamin, and Bagus Widhi Dharma S.; formal analysis, Syarifatul Ulfah and Bagus Widhi Dharma S.; investigation, Syarifatul Ulfah and Muhamad Yamin; resources, Syarifatul Ulfah; data curation, Syarifatul Ulfah, Muhamad Yamin, and Bagus Widhi Dharma S.; writing—original draft preparation, Syarifatul Ulfah; writing—review and editing, Syarifatul Ulfah, Muhamad Yamin, and Bagus Widhi Dharma S.; visualization, Syarifatul Ulfah and Bagus Widhi Dharma S.; supervision, Syarifatul Ulfah; project administration, Syarifatul Ulfah; funding acquisition, Syarifatul Ulfah. Syarifatul Ulfah served as the corresponding author. All authors have read and agreed to the published version of the manuscript.

Funding

This research was funded by the Ministry of Higher Education, Science, and Technology of the Republic of Indonesia (Kementerian Pendidikan Tinggi, Sains, dan Teknologi) through the Fundamental Research – Beginner Lecturer Research (Penelitian Dosen Pemula/PDP) scheme under Contract Number 287/C3/DT.05.00/PL-BARU/2026.

Conflicts of Interest

The authors declare no conflict of interest. This research was funded under the Penelitian Dosen Pemula (PDP) Scheme, Contract Number 287/C3/DT.05.00/PL-BARU/2026. The funding agency had no involvement in the study design; data collection, analysis, or interpretation; manuscript preparation; or the decision to submit the article for publication.

References

Adhikari, S. R., Molnar, S., & Wang, J. (2023). Seismic microzonation mapping of Greater Vancouver based on various site classification metrics. *Frontiers in Earth Science*, *11*(August), 1–11. https://doi.org/10.3389/feart.2023.1221234

Akbar, D., Rosid, M. S., & Darmanto, A. N. (2024). Seismic Vulnerability Distribution in the Central Area of Surabaya City. *Jurnal Penelitian Pendidikan IPA*, *10*(3), 1167–1174. https://doi.org/10.29303/jppipa.v10i3.6761

Aki, K. (1957). Space and time spectra of stationary stochastic waves, with special reference to microtremors. *Bulletin of the Earthquake Research Institute*, *35*, 415–456. Retrieved from http://repository.dl.itc.u-tokyo.ac.jp/dspace/handle/2261/11892

Akkaya, İ. (2020). Availability of seismic vulnerability index (K g) in the assessment of building damage in Van, Eastern Turkey. *Earthquake Engineering and Engineering Vibration*, *19*(1), 189–204. https://doi.org/10.1007/s11803-020-0556-z

Building Seismic Safety Council (BSSC). (2000). *1994 Edition: NEHRP Recommended Provisions for Seismic Regulations for New Buildings (FEMA 222A)*. Federal Emergency Management Agancy (FEMA).

Byrdina, S., Friedel, S., Vandemeulebrouck, J., Budi-Santoso, A., Suhari, Suryanto, W., Rizal, M. H., Winata, E., & Kusdaryanto. (2017). Geophysical image of the hydrothermal system of Merapi volcano. *Journal of Volcanology and Geothermal Research*, *329*, 30–40. https://doi.org/10.1016/j.jvolgeores.2016.11.011

Caesario, D., Aulia, B., Maiyudi, R., Khorniawan, W. B., & Jayanti, A. G. R. (2024). An Understanding of Volcanic Deposits With Two Dimensional Electrical Resistivity Imaging Survey at Talamau Mountain West Pasaman, Indonesia. *Sumatra Journal of Disaster, Geography and Geography Education*, *8*(1), 37–45. https://doi.org/10.24036/sjdgge.v8i1.596

Cho, I. (2023). Spatial autocorrelation method for simple microtremor array survey at rock/stiff-soil sites. *Geophysical Journal International*, *233*(2), 1296–1317. https://doi.org/10.1093/gji/ggac522

Darisma, D., Fernanda, F., & Syukri, M. (2020). Investigation of Groundwater Potential using Electrical Resistivity Method and Hydraulic Parameters in Lam Apeng, Aceh Besar, Indonesia. *Journal of Geoscience, Engineering, Environment, and Technology*, *5*(4), 211–218. https://doi.org/10.25299/jgeet.2020.5.4.5501

Fadilah, F., Simarmata, M., Farid, M., & Sukisno, S. (2025). Estimation of Sustained Groundwater Resource Potential by Analyzing Aquifer Depth Lithology in Selebar Subdistrict, Bengkulu. *Jurnal Penelitian Pendidikan IPA*, *11*(11), 1143–1150. https://doi.org/10.29303/jppipa.v11i11.12799

Fadillah, A., Harijoko, A., Hendrayana, H., Wibowo, H. E., Baud, B., Lachassagne, P., Muhammad, A. S., & Dörfliger, N. (2023). Hydrogeological Interpretation Using Electrical Resistivity Tomography: Methodology and Conceptual Model in Andesitic Volcanic Context. *International Journal of GEOMATE*, *24*(106), 25–36. https://doi.org/10.21660/2023.106.3728

Fazriati, E., Purnama, A., Algifari, G. A., Muslimah, I. S. A., Sumanto, F. H. P., Kirana, K. H., & Susanto, K. (2022). Cross-Section Resistivity Detection of Tree (Swietenia Magahoni and Gmelina) Using ERT Method. *Jurnal Penelitian Pendidikan IPA*, *8*(1), 39–44. https://doi.org/10.29303/jppipa.v8i1.965

Ferdy, F., Pandara, D. P., Bobanto, M. D., & Mambu, B. B. (2025). Characterization of Seawater Intrusion into Groundwater Aquifers Using the Electrical Resistivity Method in the Coastal Area of Tateli, North Sulawesi. *Jurnal Penelitian Pendidikan IPA*, *11*(10), 32–40. https://doi.org/10.29303/jppipa.v11i10.12303

Foti, S., Hollender, F., Garofalo, F., Albarello, D., Asten, M., Bard, P. Y., Comina, C., Cornou, C., Cox, B., Di Giulio, G., Forbriger, T., Hayashi, K., Lunedei, E., Martin, A., Mercerat, D., Ohrnberger, M., Poggi, V., Renalier, F., Sicilia, D., & Socco, V. (2018). Guidelines for the good practice of surface wave analysis: a product of the InterPACIFIC project. *Bulletin of Earthquake Engineering*, *16*(6), 2367–2420. https://doi.org/10.1007/s10518-017-0206-7

Gao, Q., Shang, Y., Hasan, M., Jin, W., & Yang, P. (2018). Evaluation of a weathered rock aquifer using ERT method in South Guangdong, China. *Water (Switzerland)*, *10*(3). https://doi.org/10.3390/w10030293

Gemilang, R., Syawalia, N., Resta, I. L., Adhitya, B., Efendi, A., Sitompul, J., Rizky Marpaung, A., & Setiawan, R. A. (2024). Identification of Site Class Using Microtremor Hvsr Measurements in Tanah Kampung District. *Journal Online of Physics*, *9*(3), 60–65. https://doi.org/10.22437/jop.v9i3.36098

Ghione, F., Köhler, A., Dichiarante, A. M., Aarnes, I., & Oye, V. (2023). Vs30 and depth to bedrock estimates from integrating HVSR measurements and geology-slope approach in the Oslo area, Norway. *Frontiers in Earth Science*, *11*. https://doi.org/10.3389/feart.2023.1242679

Hall, R., & Smyth, H. R. (2008). Cenozoic arc processes in Indonesia: Identification of the key influences on the stratigraphic record in active volcanic arcs. *Special Paper of the Geological Society of America*, *436*, 27–54. https://doi.org/10.1130/2008.2436(03)

Hanatha, F. D., Indriatmoko, T. W., & Qurrotu'aeni, W. S. (2023). Analysis of Soil and Rock Strength Using Vs30 Value and Ground Shear Strain Based on Microtremor Data in the Pindul Cave Area, Gunung Kidul, Yogyakarta. *Jurnal Geosaintek*, *9*(1), 29. https://doi.org/10.12962/j25023659.v9i1.16257

Harmoko, U., Yuliyanto, G., Nurwidyanto, I., & Widada, S. (2026). Subsurface Instability Characterization Using the Microtremor HVSR Method for Landslide Risk Assessment in Sriharjo Village, Bantul, Yogyakarta, Indonesia. *Jurnal Penelitian Pendidikan IPA*, *11*(12), 1106–1115.

https://doi.org/10.29303/jppipa.v11i12.13313

Harsuko, M. R. C., Z., Z., Nugraha, A. D., Muzli, M., Sahara, D. P., Puspito, N. T., Husni, Y. M., Prabowo, B. S., & Sarjan, A. F. N. (2020). Analysis of H/V Ratio Curve to Estimate Seismic Hazard Vulnerability in Lombok Island, West Nusa Tenggara, Indonesia. *Jurnal Geofisika*, *18*(1), 1. https://doi.org/10.36435/jgf.v18i1.432

Hayashi, K., Asten, M. W., Stephenson, W. J., Cornou, C., Hobiger, M., Pilz, M., & Yamanaka, H. (2022). Microtremor array method using spatial autocorrelation analysis of Rayleigh-wave data. *Journal of Seismology*, *26*(4), 601–627. https://doi.org/10.1007/s10950-021-10051-y

Kadri, M., Tampubolon, T., Hutahaean, J., Muztaza, N. M., & Nordin, M. N. M. (2025). Utilizing of Geophysical Methods for Geothermal Exploration at Guru Kinayan Village, Tanah Karo Regency. *Jurnal Penelitian Pendidikan IPA*, *11*(1), 367–373. https://doi.org/10.29303/jppipa.v11i1.9881

Karagoz, O., Chimoto, K., Citak, S., Ozel, O., Yamanaka, H., & Hatayama, K. (2015). Estimation of shallow S-wave velocity structure and site response characteristics by microtremor array measurements in Tekirdag region, NW Turkey. *Earth, Planets and Space*, *67*(1). https://doi.org/10.1186/s40623-015-0320-1

Karimah, K., Susilo, A., Suryo, E. A., Rofiq, A., & Hasan, M. F. R. (2022a). 3D Modelling of Geoelectrical Resistivity Data to Determine the Direction of Landslides in Kastoba Lake, Bawean Island, Indonesia. *Jurnal Penelitian Pendidikan IPA*, *8*(3), 1495–1502. https://doi.org/10.29303/jppipa.v8i3.1714

Karimah, K., Susilo, A., Suryo, E. A., Rofiq, A., & Hasan, M. F. R. (2022b). Analysis of Potential Landslide Areas Using Geoelectric Methods of Resistivity in The Kastoba Lake, Bawean Island, Indonesia. *Jurnal Penelitian Pendidikan IPA*, *8*(2), 660–665. https://doi.org/10.29303/jppipa.v8i2.1414

Keskinsezer, A., & Dağ, E. (2019). Investigating of soil features and landslide risk in Western-Atakent (Ä°stanbul) using resistivity, MASW, Microtremor and boreholes methods. *Open Geosciences*, *11*(1), 1112–1128. https://doi.org/10.1515/geo-2019-0086

Lech, M., Skutnik, Z., Bajda, M., & Markowska-Lech, K. (2020). Applications of electrical resistivity surveys in solving selected geotechnical and environmental problems. *Applied Sciences (Switzerland)*, *10*(7). https://doi.org/10.3390/app10072263

Loke, M. H., Chambers, J. E., Rucker, D. F., Kuras, O., & Wilkinson, P. B. (2013). Recent developments in the direct-current geoelectrical imaging method. *Journal of Applied Geophysics*, *95*, 135–156. https://doi.org/10.1016/j.jappgeo.2013.02.017

Longo, V., Testone, V., Oggiano, G., & Testa, A. (2014). Prospecting for clay minerals within volcanic successions: Application of electrical resistivity tomography to characterise bentonite deposits in northern Sardinia (Italy). *Journal of Applied Geophysics*, *111*, 21–32. https://doi.org/10.1016/j.jappgeo.2014.09.014

Mangga, S. A., Atmawinata, S., Hermanto, B., Setyogroho, B., & Amin, T. C. (1994). Peta Geologi Lembar Lombok Nusa Tenggara Barat. In *Pusat Survey Geologi*. Pusat Penelitian dan Pengembangan Geologi. Bandung.

Omar, J. H., Ahmad, N., Jelani, J., Suif, Z., & Othman, M. (2023). Geophysical Investigation of Groundwater Resources Using Electrical Resistivity and Induced Polarization Method. *International Journal of GEOMATE*, *25*(107), 235–242. https://doi.org/10.21660/2023.107.s8510

Pazzi, V., Di Filippo, M., Di Nezza, M., Carlà, T., Bardi, F., Marini, F., Fontanelli, K., Intrieri, E., & Fanti, R. (2018). Integrated geophysical survey in a sinkhole-prone area: Microgravity, electrical resistivity tomographies, and seismic noise measurements to delimit its extension. *Engineering Geology*, *243*, 282–293. https://doi.org/10.1016/j.enggeo.2018.07.016

Perrone, A., Lapenna, V., & Piscitelli, S. (2014). Electrical resistivity tomography technique for landslide investigation: A review. *Earth-Science Reviews*, *135*, 65–82. https://doi.org/10.1016/j.earscirev.2014.04.002

Pramono, S., Prakoso, W. A., Rohadi, S., Karnawati, D., Permana, D., Prayitno, B. S., Rudyanto, A., Sadly, M., Sakti, A. P., & Octantyo, A. Y. (2020). Investigation of Ground Motion and Local Site Characteristics of the 2018 Lombok Earthquake Sequence. *International Journal of Technology*, *11*(4), 743–753. https://doi.org/10.14716/ijtech.v11i4.3302

Prayitno, B. S., Nugraha, A. D., Zulfakriza, Z., Ridwan, M., Santoso, E., & Persada, Y. D. (2026). Seismic Site Characterization and Vs30 Mapping in Semarang City, Indonesia using Multichannel Analysis of Surface Waves. *New Zealand Journal of Geology and Geophysics*, *69*(1). https://doi.org/10.1002/jgo2.70021

Ryanto, T. A., Iswanto, E. R., Sunarko, Suryanto, S., Suntoko, H., Yuliastuti, & Susiati, H. (2022). Site characterization study with microtremor data: A case study at the West Borneo NPP potential site. *Near Surface Geophysics*, *20*(5), 531–543. https://doi.org/10.1002/nsg.12233

Sanny, T. A., Asrib, M. L., & Insani, A. Z. M. (2023). Karakterisasi tanah menggunakan pendekatan

Electrical Resistivity Tomography (ERT) pada lahan non tipikal Ipomoea Batatas "Cilembu." *Jurnal Penelitian Pendidikan IPA*, *9*(8), 6128–6135. https://doi.org/10.29303/jppipa.v9i8.4653

Subedi, B., Kiyono, J., Furukawa, A., Ono, Y., Ornthammarath, T., Kitaoka, T., Charatpangoon, B., & Latcharote, P. (2021). Estimation of Ground Profiles Based on Microtremor Survey in the Bangkok Basin. *Frontiers in Built Environment*, *7*. https://doi.org/10.3389/fbuil.2021.651902

Susilo, A., Juwono, A. M., Aprilia, F., Hisyam, F., Rohmah, S., & Hasan, M. F. R. (2023). Subsurface Analysis Using Microtremor and Resistivity to Determine Soil Vulnerability and Discovery of New Local Fault. *Civil Engineering Journal (Iran)*, *9*(9), 2286–2299. https://doi.org/10.28991/CEJ-2023-09-09-014

Susilo, A., Suryo, E. A., Fitriah, F., Sutasoma, M., & Bahtiar. (2018). Preliminary study of landslide in Sri Mulyo, Malang, Indonesia using resistivity method and drilling core data. *International Journal of Geomate*, *15*(48), 161–168. https://doi.org/10.21660/2018.48.59471

Syahdilla, M. I., Anggraeni, F. K. A., & Prihandono, T. (2024). Application of Resistivity Geoelectric Method for Predicting Subsurface Lithology At Alas Kota Site. *Jurnal Geosaintek*, *10*(3), 234–241. https://doi.org/10.12962/j25023659.v10i3.2140

Telford, W. M., Geldart, L. P., & Sheriff, R. E. (1990). *Applied geophysics*. Cambridge University Press.

Ulfah, S., Marzuki, M., & Susilo, A. (2021). Analysis Vulnerability Disaster of Landslide in Lantan Village Using Geoelectric Data and Sentinel Image. *Jurnal Penelitian Pendidikan IPA*, *7*(4), 794–801. https://doi.org/10.29303/jppipa.v7i4.915

Xie, J., Li, K., Li, X., An, Z., & Wang, P. (2023). VS30-based relationship for Chinese site classification. *Engineering Geology*, *324*. https://doi.org/10.1016/j.enggeo.2023.107253

Żogała, B., Stan-Kłeczek, I., & Waligóra, J. (2026). The electrical resistivity tomography as a tool for groundwater prospecting in the flysch lithologies: a case study from Poland. *Acta Geophysica*, *74*(1). https://doi.org/10.1007/s11600-025-01746-8